Journal of Photochemistry and Photobiology A: Chemistry 220 (2011) 102–112

Contents lists available at ScienceDirect

Journal of Photochemistry and Photobiology A: Chemistry

journal homepage: www.elsevier.com/locate/jphotochem

Photo-spectroscopic properties of benzothiadiazole-containing pendant polymers for photovoltaic applications

M. Häussler[a], S.P. King[c], M.P. Eng[c], S.A. Haque[c], A. Bilic[b], S.E. Watkins[a], G.J. Wilson[a], M. Chen[a], A.D. Scully[a,*]

[a] CSIRO Materials Science and Engineering, Bayview Avenue, Clayton, VIC 3168, Australia
[b] CSIRO Mathematics, Information and Statistics, Bayview Avenue, Clayton, VIC 3168, Australia
[c] Department of Chemistry, Imperial College London, London SW72AZ, UK

ARTICLE INFO

Article history:
Received 7 December 2010
Received in revised form 28 March 2011
Accepted 31 March 2011
Available online 8 April 2011

Keywords:
Organic photovoltaic
Block copolymer
Pendant chromophore
Benzothiadiazole

ABSTRACT

The photophysics of a homopolymer containing pendant phenoxy-benzothiadiazole-bis(thiophene) (OPhBTDT2) moieties, a block copolymer containing both OPhBTDT2 and triphenylamine-based (TPA) pendant units, and a benzothiadiazole model compound, were investigated using steady-state and time-resolved photo-spectroscopic techniques, and quantum mechanical calculations. Electronic excitation of the OPhBTDT2 chromophores leads to rapid intra-molecular charge re-distribution in the lowest unoccupied molecular orbital resulting in substantially increased electron density on the BTD component. In dilute fluid solution, the fluorescence lifetime of the OPhBTDT2 moieties in the block co-polymer was partially quenched due to photo-oxidation of TPA. The triplet excited-state lifetime of the OPhBTDT2 groups in the block co-polymer in solution was unaffected by the TPA moieties signifying that triplet excited-state OPhBTDT2 groups do not oxidize the TPA moieties. In spin-cast films, the OPhBTDT2 singlet and triplet excitons are shorter-lived than the corresponding excited states of the polymers or the OPhBTDT2 model compound in dilute solution, and the lifetimes are essentially independent of the presence of the TPA groups in the block co-polymer. This quenching of OPhBTDT2 exciton lifetimes in the films suggests efficient non-radiative energy migration to low-energy traps, possibly non-emissive OPhBTDT2 molecular aggregates. The complete quenching of fluorescence from OPhBTDT2 in a 1:1 blend of the OPhBTDT2 homoplymer and the electron acceptor [6,6]-phenyl C_{61} butyric acid methyl ester ($PC_{61}BM$) is attributed to efficient photo-induced reduction of $PC_{61}BM$ by OPhBTDT2 singlet excitons based on evidence for radical ion formation obtained from nanosecond transient absorbance measurements. The decay kinetics of the absorbance by the resulting charge carriers is consistent with a slow, trap-limited bimolecular recombination mechanism, so the low performance of photovoltaic devices produced using the blend is thought to be limited by extensive phase separation and/or low hole mobility.

1. Introduction

Organic photovoltaic (OPV) devices are currently an active focus of research among scientific and industrial researchers as they offer the potential of clean and sustainable energy generation from components that are inexpensive and easy to process. Typical OPV cells consist of an active layer fabricated from a blend of conjugated light-absorbing polymer as the electron donor and a fullerene derivative as the electron acceptor. The critical charge-separating step occurs at the interface between donor and acceptor via a photo-induced electron-transfer. The charges are subsequently transported in each homogenous phase to the corresponding electrodes. In order to achieve efficient charge separation and collection, the interfacial area between the two materials needs to be maximized while preserving the continuity of the pathways for the generated charges through a bi-continuous network such as a bulk hetero-junction (BHJ).

Such BHJ morphology is usually produced by blending the donor and acceptor materials followed by a temperature or solvent–vapour annealing step utilizing the thermodynamic driving force of complete phase separation. However, end-user devices exposed to direct sunshine are expected to experience elevated temperatures, which will induce morphological changes in their active layer causing OPV device performance to deteriorate or even fail over time. Approaches to stabilizing the active organic layer include cross-linking, addition of additives and the use of block copolymers. Block copolymers are particular attractive as their morphology can be controlled simply by varying the block-lengths. If built from suitable donor and acceptor building blocks

* Corresponding author at: CSIRO Materials Science and Engineering, Private Bag 10, Clayton MDC, VIC 3168, Australia. Tel.: +61 03 9545 2565; fax: +61 03 9545 2589.
E-mail address: andrew.scully@csiro.au (A.D. Scully).

1010-6030/$ – see front matter.
doi:10.1016/j.jphotochem.2011.03.026

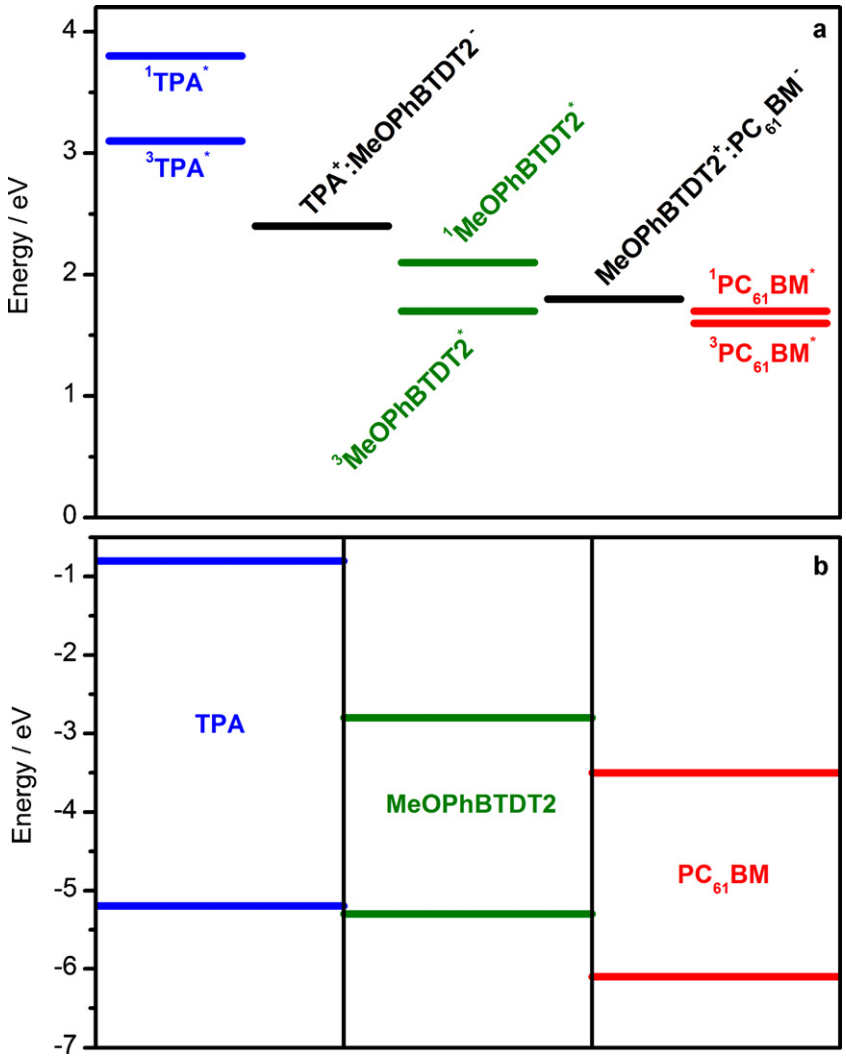

Fig. 1. (a) The energies of the first singlet excited-state and triplet excited-state together with the charge separated state energies (without Coulomb binding), and (b) the one-electron oxidation and reduction (HOMO and LUMO, respectively) energies, calculated for the investigated compounds.

they can be used either as a single-component active layer or as a kind of 'surfactant' stabilizing the BHJ morphology of the blend at the thermodynamic minimum. Results have been reported [1] that demonstrate the superior performance of block copolymer-modified active layers.

The use of electro-active pendant monomers in combination with a living polymerization technique is an elegant approach to obtaining well-defined block-copolymers. For example, the end-groups of regioregular poly-3-hexylthiophene (rr-P3HT) can be easily chemically modified with a wide variety of end-groups [2]. This gives access to a large number of controlled polymerization techniques such as ring-opening metathesis and living free-radical polymerizations [3–10]. Block copolymers consisting of rr-P3HT and perylene diimide (PDI) pendant groups have been used as a compatibiliser in blends of rr-P3HT and PDI resulting in enhanced OPV device performance [11]. Other electro-active pendant polymers used in a similar way, include building blocks such as triphenylamine (TPA), poly(phenylene vinylene) (PPV), and oligothiophenes [12–14].

Like PDI, benzothiadiazole (BTD) is also a strong electron-acceptor and thus an attractive building block for electro-active small molecules and polymers applicable in the field of organic thin film transistors, light emitting diodes, and photovoltaic devices [15–17]. We have previously designed and synthesized asymmetrically substituted BTD-containing vinyl monomers and polymerized them into homo-polymers and block co-polymers under the control of a reversible addition-fragmentation chain-transfer (RAFT) agent [18]. The resulting polymers showed tuneable absorption and emission spectra depending on their molecular architecture and exhibited efficient energy and/or electron transfer between the two pendants. The block copolymers also affected the morphology of spin-cast films and displayed rectifying behaviour in organic photovoltaic devices upon mixing with $PC_{61}BM$. In the present work, the photo-physical properties of some of these materials (shown in Scheme 1) were investigated and the results are discussed with a particular emphasis on their potential use in OPV devices.

2. Experimental

2.1. Materials

The details of the procedures used for the preparation of the model compounds 4-(5′-hexyl-2,2′-bithiophen-5-yl)-7-(4-methoxyphenyl)-2,1,3-benzothiadiazole (MeOPhBTDT2) and the polymers Poly(StOPhBTDT2), Poly(TPA), and Poly(StOPhBTDT2-*b*-TPA) are reported elsewhere [18]. Triphenylamine (TPA) (Fluka) and [6,6]-phenyl C_{61} butyric acid methyl ester ($PC_{61}BM$) (Nano-C) were used as received. Solvents used for absorption and fluores-

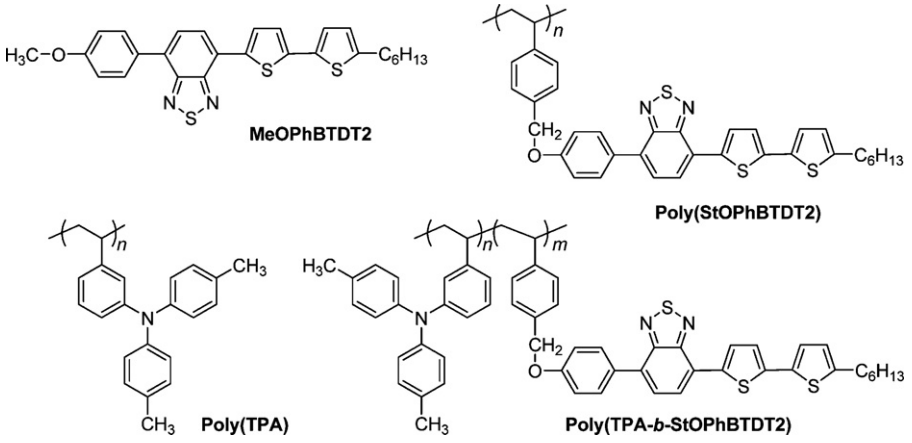

Scheme 1. Structures of benzothiadiazole-containing model compound and electro-active pendant polymers.

cence measurements were spectroscopic grade and solutions were de-gassed by bubbling with argon or nitrogen for at least 5 min prior to spectroscopic measurements, unless stated otherwise. Polymer films were prepared by spin-coating chloroform solutions of the model compounds or the polymers (10 mg/cm^3) onto UV/ozone-cleaned glass slides at spin speeds in the range 1000–4000 rpm for 60 s.

2.2. Steady-state photo-spectroscopy

UV–visible absorption spectra and steady-state photoluminescence spectra of solutions in 1 cm pathlength quartz cuvettes were measured using a UV Cary 5E spectrophotometer and a Perkin Elmer LS50 luminescence spectrometer, respectively. The optical density of solutions used for fluorescence measurements were less than 0.15 at the excitation wavelength. UV–visible absorption spectra and steady-state photoluminescence spectra of spin-cast films were measured using a Shimadzu UV-1601 spectrophotometer and a Horiba Jobin Yvon Fluorolog-3 fluorimeter, respectively. Solutions and films were not de-oxygenated for these measurements. Triplet-state energy levels were determined from total luminescence spectra of solutions measured using a Perkin Elmer LS50 luminescence spectrometer fitted with the low-temperature luminescence accessory for measurements at liquid nitrogen temperature after one flash with a delay and a gate time of 50 ns and 0.5 ms, respectively.

2.3. Kinetic photo-spectroscopy

Time-resolved photoluminescence measurements were made using commercially available time-correlated single-photon counting luminescence spectrometers (Edinburgh Instruments Ltd., FLSP920 for degassed solutions; Horiba Jobin Yvon, Fluorocube for films in air). Both systems comprised a pulsed diode laser excitation source operating at 467 nm (1 MHz repetition rate; ~0.3 ns instrument response time), and the average excitation power for measurements of photoluminescence from films was 80 μW cm^{-2}. Photoluminescence was detected using a grating monochromator.

Transient absorption spectroscopic (TAS) measurements of solutions were made using a commercially available spectrometer (Edinburgh Instruments Ltd., LP920), coupled with a nanosecond pulsed excimer laser (Lambda Physik, LPX105i) operating at 351 nm and 1 Hz repetition rate as the excitation source. The excitation energy per laser pulse at the sample was 0.9 mJ/cm^2 and the laser pulse-width was around 15 ns. All solutions used for transient absorption measurements had an optical density of ~1 at 351 nm and were de-oxygenated immediately prior to measurements by bubbling with argon for around 10 min.

Transient absorption data of spin-cast films under nitrogen were collected using a highly sensitive microsecond absorption system. Data was collected using an excitation wavelength of 450 nm, with laser pulse-width of 0.6 ns and pulse energy density in the range 45–75 μJ cm^{-2} at 4 Hz repetition rate from a dye laser (Photon Technology International Inc., GL-301) pumped by a nitrogen laser (Photon Technology International Inc., GL-3300). Samples were probed using a quartz halogen lamp (Bentham, IL1) with a stabilized power supply (Bentham, 605). Probe light was detected by a silicon photodiode and the signal subsequently amplified and passed by electronic band-pass filters to improve signal to noise. Film samples were prepared in a nitrogen glove-box and maintained in an anaerobic environment throughout the measurement.

2.4. Quantum mechanical calculations

All quantum chemical calculations were performed using the B3LYP functional. The 6-31+G(d) basis set was used for calculation of the orbitals shown in Fig. 2. For all other calculations the geometry optimizations the 6-31G(d) basis set was used without consideration of solvation effects. The HOMO and LUMO energies were calculated using the 6-311+G(d,p) basis set and solvation effects were approximated using the polarizable conductor calculation model (CPCM) [19]. Firstly, the neutral, singly oxidized, and singly reduced molecules were optimized using the smaller basis set. The resulting geometries were then used for energy calculations using the larger basis set taking solvation effects into account. This method has been shown to predict the redox properties of a large set of conjugated molecules in solution with good reproducibility [20]. Excited singlet and triplet state energies were calculated using time-dependent DFT (TD-DFT) using the same basis set and functional as for the geometry optimizations, and the non-equilibrium version [21] of CPCM, previously found to reproduce the absorption spectra of large conjugated molecules in solution [22]. To approximate the dielectric properties in the solid films the solvent toluene was used (predefined in the Gaussian 03 software) with two dielectric parameters tweaked to simulate the properties of the solid; $\varepsilon_\infty = 3.6$ and $\varepsilon = 4.5$.

2.5. Energy level measurements

The methods used for Photoelectron Spectroscopy in Air (PESA) and cyclic voltammetry measurements were the same as those described previously [18].

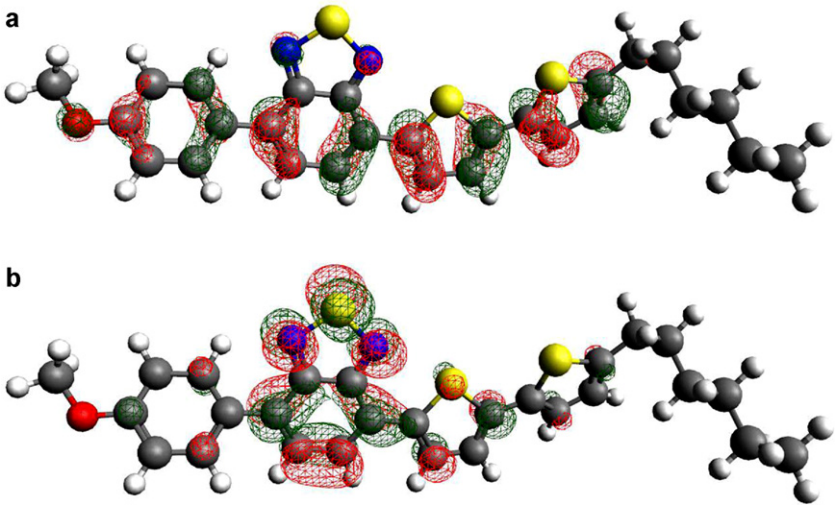

Fig. 2. Two of the calculated Kohn–Sham (KS) orbitals representing the (a) HOMO and (b) LUMO for the model compound MeOPhBTDT2 super-posed on its optimised ground-state geometry, calculated at B3LYP/6-31+G(d) level of DFT.

3. Results and discussion

3.1. Electronic characterisation

The energies of the highest-occupied molecular orbital (HOMO) and the lowest-unoccupied molecular orbital (LUMO) of the model compound MeOPhBTDT2 and triphenylamine (TPA) obtained from cyclic voltammetry measurements and from quantum mechanical calculations are given in Table 1. The energies of the triplet excited states of MeOPhBTDT2 and TPA were obtained from low-temperature phosphorescence spectra and these are also given in Table 1. The energy values for these model compounds obtained from experiment and computation were found to be in satisfactory agreement, and the energy-level diagram associated with the model compounds and $PC_{61}BM$, based on the energies obtained from computation, is shown in Fig. 1. The concept underpinning the design of the pendant polymers used in this work can be seen from this energy-level diagram which shows that in a 3-component system comprising TPA, MeOPhBTDT2 and $PC_{61}BM$, photo-induced excitation of an electron from the S_0 state (HOMO) of MeOPhBTDT2 to its S_1 state (LUMO) would, in principle, be expected to lead to transfer of an electron from the LUMO of MeOPhBTDT2 to the LUMO of $PC_{61}BM$, with a concomitant transfer of an electron from the HOMO of TPA to the vacancy that develops in the HOMO of MeOPhBTDT2 upon photo-excitation.

The spatial distributions of electronic charge in the HOMO and the LUMO of MeOPhBTDT2 obtained from DFT quantum mechanical calculations are shown in Fig. 2 superposed on the energy-minimised molecular geometry for this molecule. Electron density in the HOMO is seen to be delocalised extensively throughout the conjugated region of the molecule, whereas electron density in the LUMO is transferred substantially away from the bis-thiophene and phenoxy moieties towards the benzothiadiazole moiety. This suggests that electronic photo-excitation of MeOPhBTDT2 is likely to result in a substantially higher electron density in the vicinity of the benzothiadiazole moiety than elsewhere in the molecule, assuming that the extent of any geometrical re-arrangement that might occur on electronic excitation is negligible.

3.2. Steady-state photo-spectroscopic measurements

The UV–visible absorption spectrum of MeOPhBTDT2 in dilute solution displays a band maximum at an energy that is significantly lower (*i.e.* longer wavelength) than the lowest energy band maxima of its individual bis-thiophene [23], benzothiadiazole [24] or phenoxy [25] chromophore sub-units. This is consistent with the high degree of electronic delocalisation throughout the HOMO of this molecule seen in Fig. 2. Although the UV–visible absorption spectrum of MeOPhBTDT2 in dilute solution is essentially independent of the solvent, the wavelength of maximum photoluminescence from MeOPhBTDT2 in solution displays a strong dependence on the dielectric constant of the solvent, as shown in Fig. 3. The good linear correlation obtained from analysis according to the Lippert–Mataga model [26] (Fig. S1 in Supplementary Data) is consistent with the emitting state possessing a substantially larger dipole moment than the ground state. Using the slope of the line of best-fit obtained from this analysis, and assuming an Onsager cavity radius of 0.5 nm (*i.e.* a long molecular axis of 1 nm), the change in dipole moment between the ground state (HOMO) and the luminescent state (LUMO) is estimated to be around 9 Debye. This marked increase in dipole moment of the emitting state (*i.e.* the LUMO) of MeOPhBTDT2 is consistent with the high degree of intra-molecular electronic re-distribution upon photo-excitation of this molecule that is predicted by the quantum mechanical calculations.

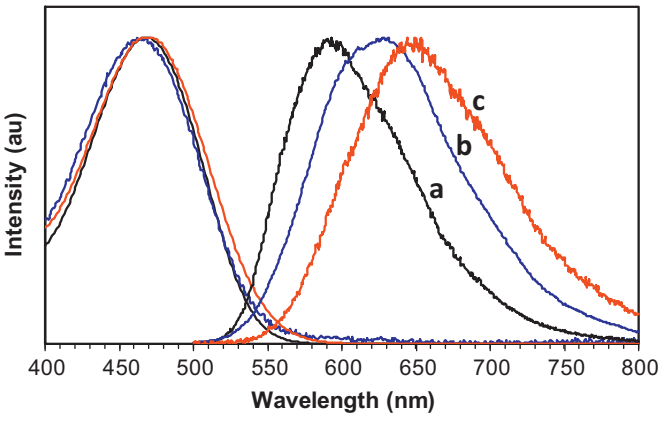

Fig. 3. Normalised UV–visible absorption spectra and photoluminescence (fluorescence) emission spectra (λ_{ex} = 470 nm) for MeOPhBTDT2 in solutions of (a) toluene (black lines), (b) dichloromethane (blue lines) and (c) dimethylsulfoxide (red lines). (For interpretation of the references to color in this figure legend, the reader is referred to the web version of the article.)

Table 1
Electronic properties of the model compounds and polymers.

	IP[a] (eV)	E_{HOMO}[b] (eV)	$E_{HOMO,DFT}$[c] (eV)	E_{LUMO}[b] (eV)	$E_{LUMO,DFT}$[c] (eV)	$E_{g,singlet}$[d] (eV)	$E_{g,triplet}$[e] (eV)
MeOPhBTDT2	−5.2	−5.4	−5.3	−3.0	−2.8	2.2	1.7
Poly(StOPhBTDT2)	−5.4	−5.3	n.d.[g]	−3.1	n.d.	2.2	n.d.
StOPhBTDT2-*b*-TPA	−5.4	−5.3	n.d.	−3.1	n.d.	2.2	n.d.
TPA	−5.7	−5.4	−5.2	−1.9[f]	−0.8	3.5	3.1
Poly(TPA)	−5.6	−5.3	n.d.	−1.9[f]	n.d.	3.4	n.d.
$PC_{61}BM$	−6.0	−5.4[h]	−6.1	−3.7	−3.5	1.7	1.6

[a] PESA measurement on spin-cast films.
[b] Calculated from cyclic voltammetry measurements of dichloromethane solutions.
[c] Calculated at B3LYP/6-31G(d)//B3LYP/6-311+G(d,p) level of DFT.
[d] Optical bandgap, calculated using low-energy onset of UV absorption of thin films.
[e] Energy gap, calculated using high-energy onset of phosphorescence from MeOPhBTDT2 and TPA in MeTHF solutions at 77 K. Value for $PC_{61}BM$ is based on the 0–0 transition at 798 nm in the phosphorescence spectrum of C_{60} in an organic glass matrix at 1.2 K (Ref. [50]).
[f] Calculated using data from columns 3 and 7, where $E_{LUMO} = E_{HOMO} + E_g$.
[g] n.d. = not determined.
[h] Calculated using data from columns 5 and 7, where $E_{HOMO} = E_{LUMO} - E_{g,singlet}$.

The UV–visible absorption spectra and photoluminescence spectra of poly(StOPhBTDT2) and StOPhBTDT2-*b*-TPA in dilute solution display no appreciable difference to those measured for MeOPhBTDT2 in solution. The absorption spectra and photoluminescence spectra of spin-cast films of these polymers are similar to those measured for a spin-cast film of MeOPhBTDT2 in that all display a Stokes' shift of about 6.14×10^3 cm^{-1} (0.76 eV), although the wavelengths of maximum absorption and luminescence for the polymer films are shifted by around 25 nm to longer wavelengths compared with the spectra of the MeOPhBTDT2 film (Fig. S2 in Supplementary Data). No evidence was found from the steady-state spectra for the presence of discrete ground-state dimers or higher-order molecular aggregates of the OPhBTDT2 chromophores in films of the model compound or the polymers.

3.3. Kinetic photo-spectroscopic measurements of dilute solutions

3.3.1. Photoluminescence decay

The decay of photoluminescence (fluorescence) from dilute chloroform solutions of MeOPhBTDT2, poly(StOPhBTDT2) and StOPhBTDT2-*b*-TPA is shown in Fig. 4 and in each case was found to be independent of the presence of dissolved oxygen. The rate of fluorescence decay from the electronically excited MeOPhBTDT2 chromophore is significantly faster for the StOPhBTDT2-*b*-TPA block co-polymer than for either the model compound or the homopolymer. Since the HOMO–LUMO band-gap energy of the TPA moiety substantially exceeds that of MeOPhBTDT2, the extent of quenching due to electronic energy transfer from the emitting state of electronically excited MeOPhBTDT2 to TPA can be assumed to be negligible. Therefore, the increased rate of photoluminescence decay observed in the case of StOPhBTDT2-*b*-TPA is attributed to the photo-induced oxidation of TPA by the electronically excited MeOPhBTDT2 molecule since, as shown in the energy-level diagram in Fig. 1, the HOMO energy of TPA is essentially iso-energetic with that of MeOPhBTDT2, implying that electron transfer from the HOMO of TPA to the vacancy in the HOMO of the electronically excited MeOPhBTDT2 molecule is energetically feasible.

The photoluminescence decay time for MeOPhBTDT2 in dilute chloroform is 7.6 ns and the absolute photoluminescence quantum yield was measured to be 0.74 ± 0.06. This indicates that the upper limit for the quantum yield of intersystem crossing to the triplet excited-state of the OPhBTDT2 chromophore is 0.26 and that the rate constant for this process is no greater than 3.4×10^7 s^{-1}. The absence of a detectable rise-time in the decay curves indicates that the rate constant for the intra-molecular charge re-distribution from the initially excited state to the emitting state is $>10^{10}$ s^{-1}.

3.3.2. Transient absorption spectroscopy

The transient absorption spectrum of MeOPhBTDT2 in dilute chloroform solution (~50 μmol dm^{-3}), measured 1 μs after laser excitation, is shown in Fig. 5. The absence of any appreciable change in spectral features with time after excitation (Fig. S3 in Supplementary Data) indicates that this spectrum is associated with absorbance by a single transient species. Furthermore, as found for the ground-state absorption spectrum of MeOPhBTDT2,

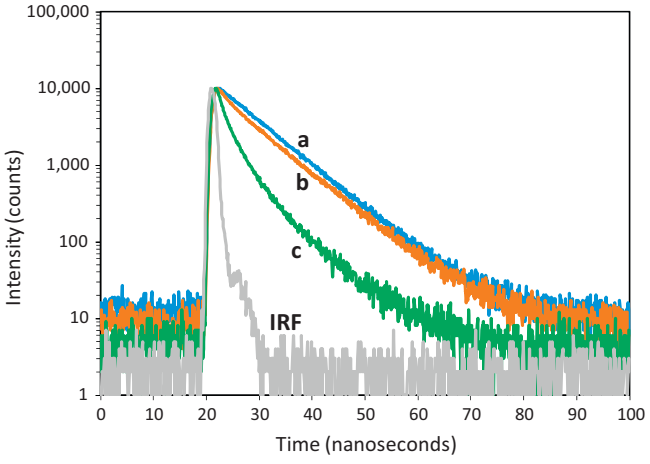

Fig. 4. Fluorescence decay of de-oxygenated chloroform solutions of: (a) MeOPhBTDT2, (b) poly(StOPhBTDT2), and (c) StOPhBTDT2-*b*-TPA. λ_{ex} = 466 nm; λ_{em} = 610 nm. IRF = instrument response function.

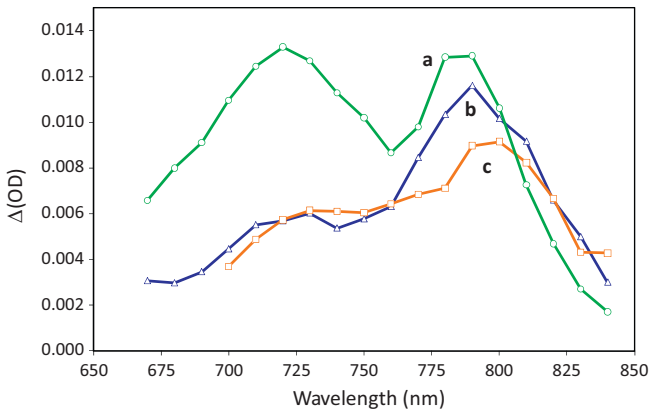

Fig. 5. Transient absorption spectra of de-oxygenated chloroform solutions recorded at 1 μs after excitation by the laser pulse: (a) MeOPhBTDT2 (gate width = 6.5 μs), (b) StOPhBTDT2-*b*-TPA (gate width = 3.5 μs), and (c) poly(StOPhBTDT2) (gate width = 3.5 μs). λ_{pump} = 351 nm.

the absorption spectrum of the transient species is distinctly different from the absorption spectra reported for the triplet excited-state [27,28] associated with the bis-thiophene chromophore sub-unit of this molecule or its radical cation [28,29] or the absorption spectrum of the radical anion of a closely related benzothiadiazole derivative [30], and attempts to measure absorption by the triplet excited-state of anisole have been fruitless [31,32]. This lack of correlation indicates that the transient absorbance is unlikely to be associated with either an excited state localised on a chromophore sub-unit of the molecule or a zwitterionic species that would result from formal excited-state intra-molecular electron-transfer. Therefore, the transient absorption observed for MeOPhBTDT2 in solution is assigned to electronic excitation of a molecular triplet excited-state of the OPhBTDT2 chromophore.

The decay of the transient absorbance at 750 nm for a chloroform solution of MeOPhBTDT2 is shown in Fig. 6. This decay was analysed using Eq. (1), and the analysis results are summarised in Table 2.

$$\Delta(\mathrm{OD})_t = A_1 e^{-k_1 t} \quad (1)$$

The good fit to the decay of the transient absorbance using this exponential function provides further evidence that the transient absorbance originates from a single transient species and indicates that quenching by triplet–triplet annihilation (TTA) [33] can be regarded as negligible under the conditions used for this measurement.

The transient absorption spectra measured for chloroform solutions of poly(StOPhBTDT2) and StOPhBTDT2-*b*-TPA are shown in Fig. 5. Again, the lack of a spectral change with time after excitation (Figs. S4 and S5 in Supplementary Data) is consistent with the existence of a single transient absorbing species and, like MeOPhBTDT2, this transient absorbance is attributed to a molecular excitation of the OPhBTDT2 chromophores in these polymers, namely the excited triplet-state. However, as seen in Fig. 6, the decay times of the transient absorption for both poly(StOPhBTDT2) and StOPhBTDT2-*b*-TPA are substantially faster than for MeOPhBTDT2 and, unlike the case of the model compound, satisfactory fits of the decay curves measured for the polymers in solution could not be obtained by analysis using Eq. (1) (Figs. S6 and S7 in Supplementary Data). The TPA chromophores in StOPhBTDT2-*b*-TPA absorb very little of the excitation radiation at 351 nm. Therefore, the extent of formation of transient absorbing species such as the triplet excited-state of TPA or radical cations of TPA upon direct excitation of this component of the block copolymer can be considered to be negligible and unlikely to be the reason for the observed non-exponential decay kinetics for the block co-polymer.

Since the pendant OPhBTDT2 chromophores in poly(StOPhBTDT2) and StOPhBTDT2-*b*-TPA are fixed to the polymer backbone, the local concentrations of these chromophores in chloroform solution might be expected to be markedly higher than that of the model compound MeOPhBTDT2 for a given bulk concentration of chromophore, especially if coiling of the polymer chains occurs in chloroform. Consequently, the local concentration of triplet excited-states of the OPhBTDT2 chromophores in poly(StOPhBTDT2) and StOPhBTDT2-*b*-TPA formed on electronic photo-excitation could be significantly higher for the polymers than for the model compound. At sufficiently high local concentrations of triplet excited-states of the OPhBTDT2 moieties in poly(StOPhBTDT2) and StOPhBTDT2-*b*-TPA it is conceivable that TTA may occur, resulting in quenching of the lifetime of the triplet excited-state. The lack of spectral evidence for the existence of multiple transient absorbing species and the non-exponentiality found in the transient absorption decays for the polymers in solution are consistent with the occurrence of TTA.

It has been demonstrated [34] that a statistical approach to describe triplet-state decay kinetics in the presence of TTA which considers the decay of triplet excitation in ensembles of closed domains (*e.g.* non-interacting polymer chains, micelles, or nanoparticles) leads to an expression involving a series of exponential terms where, to a good approximation, only the first two terms are of significance (Eq. (2)). In contrast with the standard approach to the description of triplet-state decay in the presence of TTA, which is applicable in cases where the rate of bimolecular annihilation is much slower than the intrinsic decay rate, the mathematical expression arising from the statistical approach is valid for domains with small dimensions and large TTA rate constants. Accordingly, in

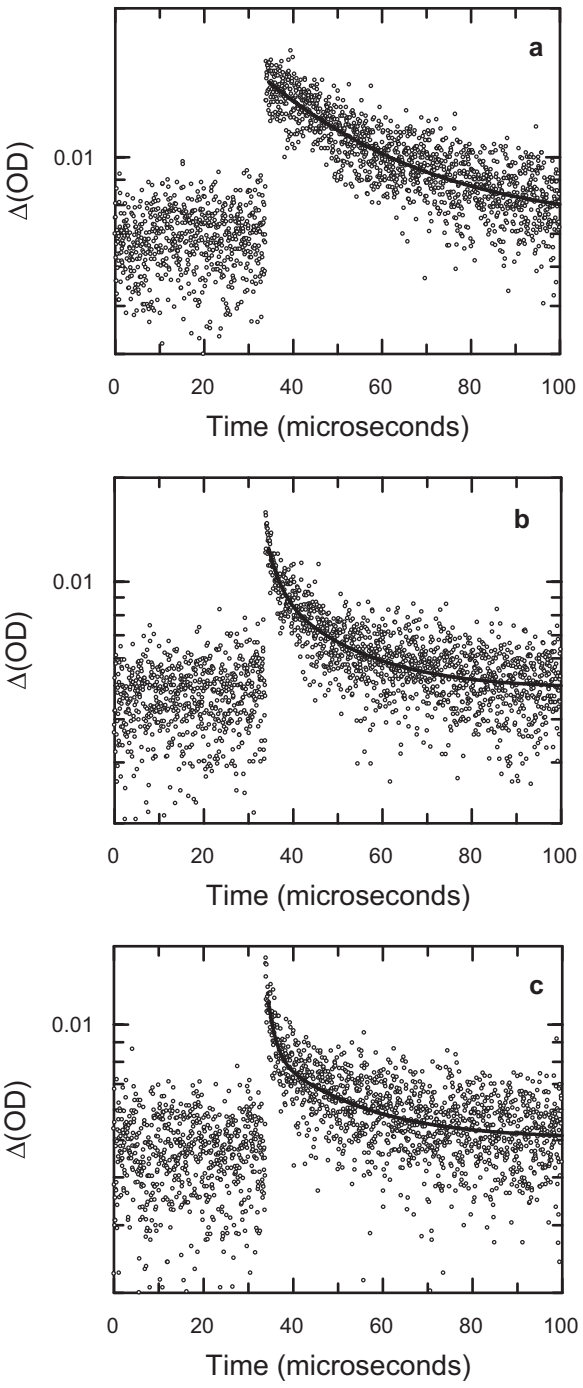

Fig. 6. Decay of transient absorbance of de-oxygenated chloroform solutions of: (a) MeOPhBTDT2, (b) poly(StOPhBTDT2) and (c) StOPhBTDT2-*b*-TPA.λ_{pump} = 351 nm; λ_{probe} = 750 nm. Solid lines are the best fits using Eq. (1) or Eq. (2), and associated values of the fitting parameters are given in Table 2. Note that the ordinate values are plotted using a logarithmic scale.

Table 2
Best-fit transient absorbance decay parameters in de-oxygenated chloroform solution or spin-cast films.

	Sample	A_1 $\times 10^{+3}$	k_1 $\times 10^{-5}$ s	A_2 $\times 10^{+3}$	β $\times 10^{-5}$ s	$\langle k \rangle$[a] $\times 10^{-5}$ s
Solution	MeOPhBTDT2[b]	7.0 ± 0.1	0.31 ± 0.02	–	–	0.31
	Poly(StOPhBTDT2)[c]	3.3 ± 0.8	0.66 ± 0.03	4.6 ± 0.6	5.9 ± 1.4	3.7
	StOPhBTDT2-b-TPA[c]	3.0 ± 0.3	0.59 ± 0.05	3.0 ± 0.3	5.3 ± 2.2	3.0
Spin-cast films	Poly(StOPhBTDT2)[c]	2.5 ± 0.1	0.98 ± 0.01	1.7 ± 0.1	3.7 ± 0.1	2.1
	StOPhBTDT2-b-TPA[c]	2.5 ± 0.1	0.50 ± 0.01	1.5 ± 0.1	3.6 ± 0.1	1.7

[a] Calculated according to: $\langle k \rangle = \frac{k_1 \beta}{\beta f_1 + k_1 f_2}$, where $f_1 = \frac{A_1 \beta}{A_1 \beta + A_2 k_1}$ and $f_2 = 1 - f_1$.
[b] Best-fit parameters obtained using Eq. (1).
[c] Best-fit parameters obtained using Eq. (2).

the presence of TTA, the transient absorption decay kinetics of the triplet excited-state species formed on electronic photo-excitation of poly(StOPhBTDT2) and StOPhBTDT2-*b*-TPA in solution should, to a good approximation, be described by Eq. (2), where $\beta = k_2 + 2k_1$.

$$\Delta(\mathrm{OD})_t = A_1 e^{-k_1 t} + A_2 e^{-\beta t} \quad (2)$$

The decay of transient absorbance at 750 nm of poly(StOPhBTDT2) and StOPhBTDT2-*b*-TPA in chloroform were found to be described well by Eq. (2) (Figs. S6 and S7 in Supplementary Data) and the analysis results are summarised in Table 2. The more slowly decaying component is assigned to the unquenched decay of the triplet excited-state of the OPhBTDT2 chromophore. Since this component accounts for around 90% of the transient absorption signal, the decay of the majority of the triplet excited-state species is not affected by quenching due to TTA, indicating that most domains contain only a single excitation under the experimental conditions used in the present work.

The transient absorption decay rates for StOPhBTDT2-*b*-TPA are essentially the same as for poly(StOPhBTDT2) indicating that the presence of the TPA block in StOPhBTDT2-*b*-TPA has little effect on the lifetime of the OPhBTDT2 triplet excited-state. This result indicates that, unlike the singlet excited-state of the OPhBTDT2 chromophores in StOPhBTDT2-*b*-TPA, in chloroform solution the triplet excited-state of these chromophores do not participate in an electron-transfer reaction with the pendant TPA moieties in the block co-polymer. The result also implies that the presence of the TPA units in the block co-polymer have little impact on the preferred conformation of the polymer chains in chloroform.

3.4. Kinetic photo-spectroscopic measurements of pristine films

The photoluminescence decay curves presented in Fig. 7 indicate that the lifetime of the fluorescent state of the OPhBTDT2 chromophore in pristine films of poly(StOPhBTDT2) and StOPhBTDT2-*b*-TPA is essentially the same as for the model compound MeOPhBTDT2. The possibility of formation of electronically excited TPA chromophores in the StOPhBTDT2-*b*-TPA film due to direct absorption of the excitation light can be disregarded because the absorption by the TPA units at this wavelength is negligibly small relative to absorption by the OPhBTDT2 chromophores. A comparison of the photoluminescence decay curves for MeOPhBTDT2 shown in Figs. 4 and 7 reveals a markedly faster fluorescence decay rate for the pristine film compared with dilute solution. A decrease in fluorescence lifetime of chromophores in highly concentrated solid-state films compared with dilute solution has been reported [35,36] for a wide variety of chromophores and is usually attributed to quenching arising from diffusion of singlet excitons to energy traps such as molecular aggregates of the chromophores having lower optical band-gap than the un-associated chromophore and which are either weakly or non-luminescent. Although no clear evidence for absorption or emission by molecular aggregates of the OPhBTDT2 moieties was found in the steady-state spectra, and despite the relatively small degree of overlap between the absorption and fluorescence spectra of the OPhBTDT2 chromophores, exciton migration within the ensemble of closely spaced OPhBTDT2 chromophores is presumed to occur with sufficient efficiency to result in some trapping of energy by molecular aggregates of OPhBTDT2 chromophores, even at relatively low trap concentrations.

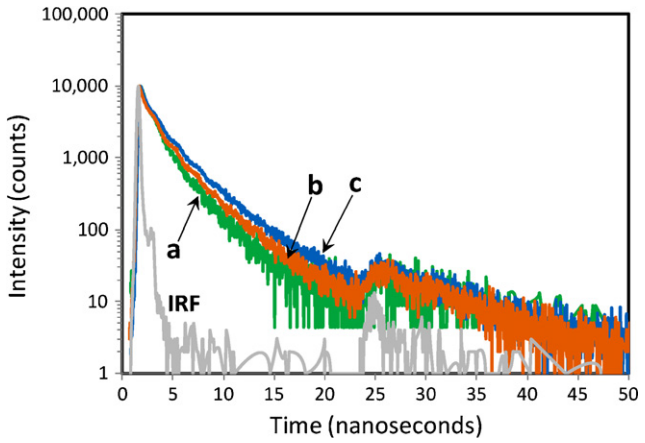

Fig. 7. Fluorescence decay of pristine films of: (a) MeOPhBTDT2, (b) poly(StOPhBTDT2), and (c) StOPhBTDT2-*b*-TPA. λ_{ex} = 467 nm; λ_{em} = 650 nm. IRF = instrument response function.

The absence of any substantial difference in the rate of photoluminescence decay from the StOPhBTDT2-*b*-TPA film compared with films of poly(StOPhBTDT2) or MeOPhBTDT2 is in contrast with the distinct quenching of the fluorescence lifetime observed for StOPhBTDT2-*b*-TPA in solution. This lack of enhanced quenching for the StOPhBTDT2-*b*-TPA film suggests that the fluorescence decay kinetics is dominated by the same processes as for films of poly(StOPhBTDT2) or MeOPhBTDT2, namely trapping of diffusing singlet excitons by molecular aggregates, with little contribution from the photo-oxidation of the TPA moieties by electronically excited OPhBTDT2 observed in dilute solution. It is possible that the slightly longer-lived photoluminescence observed for the StOPhBTDT2-*b*-TPA film might be the result of the pendant TPA moieties acting as diluents for the OPhBTDT2 chromophores, thereby lowering their propensity to form molecular aggregates.

The decay of the transient absorption at 750 nm by pristine films of poly(StOPhBTDT2) and StOPhBTDT2-*b*-TPA is shown in Fig. 8. The transient absorption decay in each case is not mono-exponential, but was found to be described satisfactorily by the bi-exponential function shown in Eq. (2) and the best-fit parameter values are summarised in Table 2. It is assumed that, as was the case for the polymers in dilute solution, the sole transient absorbing species in these films is the triplet excited-state of the OPhBTDT2 chromophores, and that the non-exponentiality of the transient absorption decay is not the result of absorption by multiple transient species. A significant increase in the decay rate of the transient absorption at 750 nm was observed when

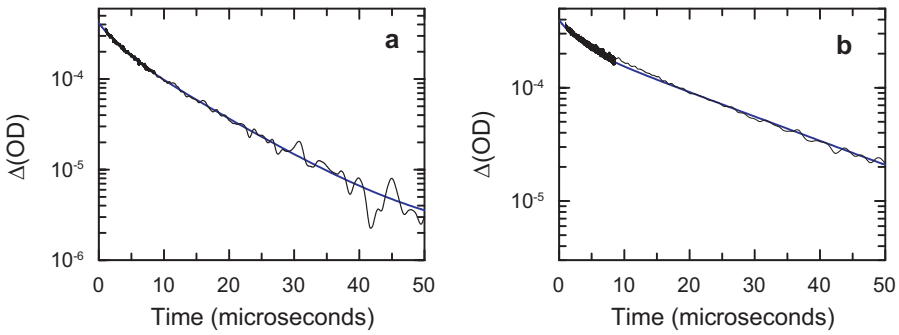

Fig. 8. Decay of transient absorbance of pristine films of (a) poly(StOPhBTDT2) and (b) StOPhBTDT2-*b*-TPA.λ_{pump} = 450 nm; λ_{probe} = 750 nm. Blue solid lines are best-fits using Eq. (2), and associated parameter values given in Table 2. (For interpretation of the references to color in this figure legend, the reader is referred to the web version of the article.)

the measurement was conducted with the sample exposed to air, which provides further strong evidence that the transient absorbing species are OPhBTDT2 chromophore triplet excitons. As seen from the data in Table 2, the mean decay rate, <k>, of the transient absorption by the StOPhBTDT2-*b*-TPA film is not enhanced compared with the poly(StOPhBTDT2) film indicating that the pendant TPA moieties do not quench the triplet excited-state of the OPhBTDT2 chromophores, as was also found for StOPhBTDT2-*b*-TPA in dilute chloroform solution.

The magnitude of the rate constant for uni-molecular decay of the triplet excited-state, k_1, obtained for the poly(StOPhBTDT2) film is significantly larger than for this polymer in dilute solution (see Table 2), whereas this value is expected to be invariant based on the physical model used for the derivation of Eq. (2). This suggests that Eq. (2) might not provide a valid physical description of the triplet-state decay kinetics for these highly concentrated solid-state film systems. Furthermore, the smaller magnitude of the mean decay constant, $\langle k \rangle$, of the excited triplet-state of OPhBTDT2 chromophores observed for the poly(StOPhBTDT2) film compared with this polymer in dilute solution is not consistent with the expectation that TTA should occur with greater efficiency at the higher molecular densities in the films. Consequently, the mean rate constants for decay of transient absorption for the homopolymer film are thought to be associated with trapping of triplet exciton energy in the molecularly dense film rather than TTA. The smaller magnitude of k_1 (*i.e.* slower uni-molecular decay of the triplet excitons) obtained for the StOPhBTDT2-*b*-TPA film compared with that for the poly(StOPhBTDT2) film provides further support for the above-mentioned idea that the TPA moieties might act as diluents for the OPhBTDT2 chromophores in the film, thereby reducing both the concentration of ground-state molecular aggregate traps and also the distance over which triplet excitons can diffuse.

3.5. Kinetic photo-spectroscopic measurements of blend films containing $PC_{61}BM$

The results of kinetic photoluminescence and transient absorption measurements of the pristine film of StOPhBTDT2-*b*-TPA described above indicate that the presence of the pendant TPA moieties is unlikely to provide significant additional benefit in terms of hole transport from the electronically excited OPhBTDT2 chromophores in an OPV device. Consequently, subsequent investigation of polymer blends comprising $PC_{61}BM$ focused on the use of the homopolymer. The decay of photoluminescence from a pristine film of poly(StOPhBTDT2), a film comprising a blend of poly(StOPhBTDT2) and $PC_{61}BM$ (50%, w/w), and a pristine film of $PC_{61}BM$ are shown in Fig. 9. The fluorescence decay kinetics for the blend was found to be essentially identical to that of a pristine film of $PC_{61}BM$ indicating effectively complete quenching of the photoluminescence from OPhBTDT2 singlet excitons by the $PC_{61}BM$.

As seen from the data in Table 1, the calculated HOMO–LUMO band-gap energy for $PC_{61}BM$ is slightly larger than that of the OPhBTDT2 chromophore, so quenching of the luminescence from the OPhBTDT2 chromophores as a result of non-radiative electronic energy transfer from OPhBTDT2 singlet excitons to ground-state $PC_{61}BM$ is not expected to be highly efficient. If it is assumed that: (i) the complete quenching of OPhBTDT2 fluorescence implies an energy transfer efficiency of close to 100%, (ii) the fluorescence quantum efficiency for the OPhBTDT2 singlet excitons in the film is around 40% that of MeOPhBTDT2 in dilute solution (based on the shorter fluorescence lifetime measured for the pristine MeOPHBTDT2 film), and (iii) the magnitude of the extinction coefficient of OPhBTDT2 chromophores (Fig. S8 in Supplementary Data) is around 20 times that of $PC_{61}BM$ at the excitation wavelength of 467 nm, the steady-state $PC_{61}BM$ fluorescence intensity detected from the film comprising the blend would be expected to be around 43% of that of a pristine film of $PC_{61}BM$ absorbing a similar fraction of excitation light. However, the steady-state $PC_{61}BM$ fluorescence detected from the blend film is only around 15% that of a pristine film of $PC_{61}BM$ absorbing a comparable fraction of the excitation light. This result indicates that essentially all of the $PC_{61}BM$ fluorescence from the blend film arises due to direct excitation of $PC_{61}BM$ chromophores rather than from non-radiative electronic energy transfer for the OPhBTDT2 singlet excitons.

Quenching of fluorescence from OPhBTDT2 singlet excitons may also occur as a result of photo-reduction of $PC_{61}BM$. The absence of detectable fluorescence from OPhBTDT2 singlet excitons in the blend implies a value of at least around $10^{10}\ s^{-1}$ for the magni-

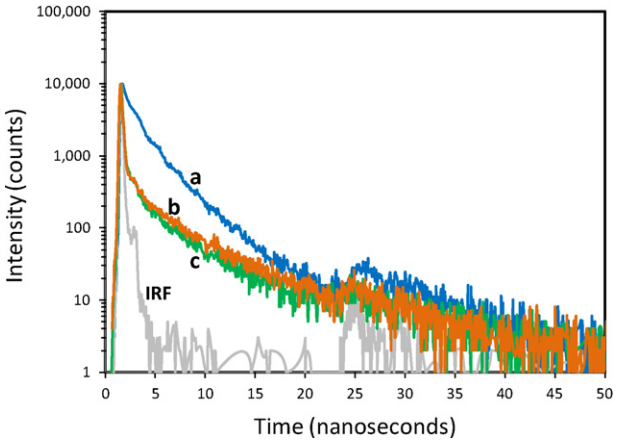

Fig. 9. Fluorescence decay of films of: (a) poly(StOPhBTDT2), (b) $PC_{61}BM$ and (c) a blend comprising poly(StOPhBTDT2) and $PC_{61}BM$ (50 wt%). λ_{ex} = 467 nm; λ_{em} = 650 nm. IRF = instrument response function.

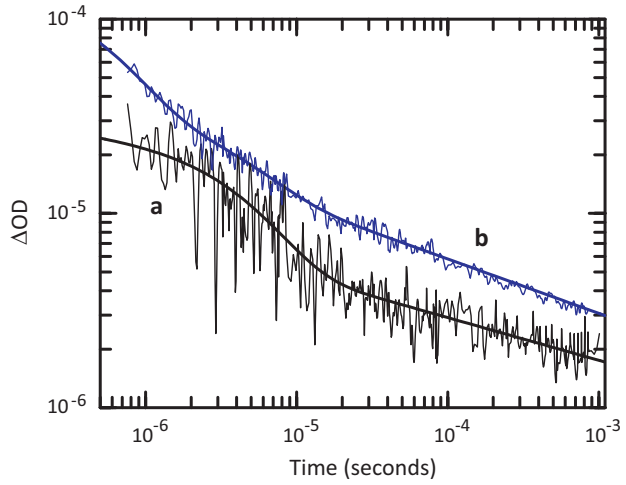

Fig. 10. Decay of transient absorbance at (a) 1070 nm and (b) 750 nm of a film comprising a blend of poly(StOPhBTDT2) and $PC_{61}BM$ (50 wt%).λ_{pump} = 450 nm. The line of best-fit for the decay of absorbance at 1070 nm was calculated using Eq. (3). See text for details of analysis of data at 750 nm.

tude of the rate constant of electron transfer from the OPhBTDT2 chromophores to $PC_{61}BM$ molecules, which is sufficiently fast to preclude formation of OPhBTDT2 triplet excitons via intersystem crossing from the corresponding singlet excitons.

The absorption spectrum of the $PC_{61}BM$ radical anion extends over wavelengths ranging from about 850 nm to 1200 nm with a maximum absorption reported to lie at 1020 nm [37], compared with the C_{60} radical anion which displays an absorption maximum at 1070 nm [38,39]. Absorption in this wavelength range by $PC_{61}BM$ triplet excitons is negligibly small [40], and so the transient absorption signal detected at 1070 nm (Fig. 10(a)) is attributed to $PC_{61}BM$ radical anions. The decay of the transient absorption at 1070 nm displays an initial fast phase that dominates the time evolution of the transient absorption decay for about 10 μs after excitation. This initial rapid decay is followed by a second phase that decays much more slowly, extending into the millisecond timescale. The lack of change in the absorption decay dynamics observed when the sample was exposed to air provides further evidence that the absorbing species is most likely to be $PC_{61}BM$ radical anions rather than triplet excitons. The slower phase of the decay at 1070 nm (>10 μs) was analysed using the power term in the expression shown in Eq. (3) which has been used to describe bimolecular recombination kinetics in several other polymer/$PC_{61}BM$ blend systems [41–44]. This function was found to provide a good fit to the decay profile, with the recovered values for the mono-exponential decay time (k^{-1}) and α from this analysis being 4.3 μs and 0.22, respectively.

$$\Delta(\mathrm{OD})_t = Ae^{-kt} + Bt^{-\alpha} \quad (3)$$

The decay of the transient absorption at 1070 nm is, therefore, ascribed to bimolecular recombination of the $PC_{61}BM$ radical anions with OPhBTDT2 polarons in which the fast decaying phase is associated with bimolecular recombination of free charge carriers generated when the density of photo-generated polarons exceeds the density of local states, and the slower decaying phase originates from bimolecular recombination of charges after thermal activation out of an exponential distribution of localised (trapped) states [41–44]. The magnitude of α found for this blend of poly(StOPhBTDT2) and $PC_{61}BM$ is at the lower end of the range of values reported [37,41,42,44,45] for other amorphous polymer/$PC_{61}BM$ blends, suggesting that the traps in this blend are relatively deep. Relaxation of photo-generated polymer polarons into these localised trap states is expected to slow the rate of bimolecular recombination in a functioning OPV device which is desirable for efficient charge-carrier collection by the electrodes. However, the efficiency of charge collection will also be determined by other factors such as the extent to which continuous charge percolation pathways exist in the blend and intrinsic charge mobility of the blend components.

The absorption spectrum of the triplet excited-state of fullerene derivatives extends over the wavelength range 600–900 nm with maximum absorption occurring typically around 700–750 nm [46,47]. The absorption maximum for $PC_{61}BM$ triplet excitons in solid films is reported to occur at around 720 nm [40]. Since the extent of formation of OPhBTDT2 triplet excitons can be assumed to be negligible, and the absorption at 750 nm by $PC_{61}BM$ radical anions is vanishingly small, the transient absorption at 750 nm measured for the film (Fig. 10(b)) is attributed to $PC_{61}BM$ triplet excitons and/or OPhBTDT2 polarons. If $PC_{61}BM$ triplet excitons are formed exclusively via intersystem crossing from the $PC_{61}BM$ singlet excitons formed by direct excitation, then the decay would be expected to be mono-exponential having a decay time of around 11 μs [40,48], in the absence of other effects. Alternatively, if $PC_{61}BM$ triplet excitons are formed in sufficiently high concentrations to result in TTA, then the function shown in Eq. (2) might be expected to provide a good description of the decay kinetics. The decay of transient absorbance at 750 nm shown in Fig. 10(b) is not mono-exponential, and could not be described successfully using the bi-exponential function shown in Eq. (2). Evidence that a significant portion of the absorbance at this wavelength arises due to species other than $PC_{61}BM$ triplet excitons comes from: (i) the inability of these functions to describe adequately the decay of absorbance at 750 nm, (ii) the presence of a very long-lived decay phase, and (iii) the lack of a detectable effect of oxygen (air) on the kinetics of the transient absorption decay at 750 nm.

As was the case for the decay of the $PC_{61}BM$ radical anions, the decay profile at 750 nm is seen to be dominated by a rapid phase that extends up until around 10 μs after excitation, after which a second much slower decay phase becomes evident. This long-lived phase, extending into the millisecond time-range, suggests that the transient absorbing species is involved in the recombination of radical ion-pairs. However, analysis of the decay using the function shown in Eq. (3) also failed to provide a satisfactory fit, providing further evidence that the absorption signal probably arises from multiple transient species.

A good fit to the data was obtained by using an empirical equation comprising a sum of two exponential terms and a power term (Fig. 10(b)), with the recovered exponential decay times being 0.5 μs and 4.5 μs, and the value for α being 0.28. The magnitudes of the longer exponential decay time and α are in good agreement with the values of the parameters obtained from analysis of the decay at 1070 nm using Eq. (3). This finding supports the hypothesis that the species predominantly responsible for the absorbance at 750 nm decays as a result of the recombination of radical ion-pairs. The lack of effect of oxygen (air) on the kinetics of the transient absorption decay at 750 nm (as was also found at 1070 nm) suggests that the species most likely to be primarily responsible for the absorbance at 750 nm is OPhBTDT2 polarons.

The origin of the more rapidly decaying component (0.5 μs lifetime) seen in Fig. 10(b) is unclear at present, but is tentatively ascribed to absorption by $PC_{61}BM$ triplet excitons. The lifetime is significantly shorter than the lifetime of 11 μs reported [40] for $PC_{61}BM$ triplet excitons in a blended film comprising the conjugated polymer poly(9,9-dioctylfluorene-*alt*-benzothiadiazole) (F8BT) and $PC_{61}BM$ (50 wt%), although the lifetime of $PC_{61}BM$ triplet excitons has been shown to decrease with increasing $PC_{61}BM$ concentration in spin-cast films [48] which was attributed to the effects of $PC_{61}BM$ clustering and fullerene–fullerene interactions. The much shorter lifetime obtained in the present work would be consistent with quenching of the $PC_{61}BM$ triplet exci-

tons if extensive separation of the $PC_{61}BM$ and poly(StOPhBTDT2) phases occurs in the blend film, and the absence of a measurable effect of oxygen on the lifetime of this short-lived component could be the result of concentration quenching effects dominating the overall decay mechanism. It is estimated that the $PC_{61}BM$ molecules in the 1:1 poly(StOPhBTDT2)/$PC_{61}BM$ blended film absorb around 5% of the excitation light at 450 nm, so intersystem crossing from the $PC_{61}BM$ singlet excitons formed upon direct excitation is one pathway for the formation of $PC_{61}BM$ triplet excitons. Alternatively, geminate recombination of radical ion-pair triplet states is another possible source for the formation of $PC_{61}BM$ triplet excitons [41].

An OPV device consisting of a blend of poly(StOPhBTDT2) and $PC_{61}BM$ (80%, w/w) was fabricated and analysed using the same methodology as described previously [18]. While the open-circuit voltage, which reflects the difference between the ionization potential of the donor and the electron affinity of the acceptor, of this device was high (0.65 V), the photo-current generated in the active layer, as measured by the power conversion efficiency (PCE), was relatively low (0.10%) despite the presence of the relatively slow bimolecular recombination pathway described above. It is possible that the low PCE value might arise due to extensive phase separation resulting in a paucity of charge percolation pathways which would also contribute to the low fill factor (0.27) found for this device. Low hole mobility in the poly(StOPhBTDT2) phase might also be a contributing factor. Recent work on block copolymer systems suggests that their major benefits to OPV are as modifiers for morphology and as stabilizers of multi-component mixtures [11,49], and work is currently underway to explore this pathway for our pendant polymers.

4. Conclusions

Electronic excitation of pendant OPhBTDT2 moieties in the polymers studied in this work leads to rapid electronic re-distribution in the LUMO resulting in a substantial shift in electron density to the benzothiadiazole component. In fluid solution, the fluorescence lifetime of this partially charge-transferred singlet excited-state of the OPhBTDT2 moiety is only partly quenched by the presence of the TPA groups in the block co-polymer, indicating photo-oxidation of TPA groups occurs to only a limited extent. In contrast, the lifetime of the triplet excited-state of the OPhBTDT2 groups in the block co-polymer remains completely unaffected by the presence of the TPA moieties, signifying that the triplet excited-state of the OPhBTDT2 groups do not participate in photo-oxidation of the pendant TPA units.

In spin-cast pristine films of the polymers, the decay of both the OPhBTDT2 singlet and triplet excitons is faster than for the corresponding excited-states of these polymers in dilute solution or for the model compound, and the presence of the TPA groups in the co-polymer has essentially no affect on these decay times. Therefore, the quenching of the OPhBTDT2 singlet and triplet excitons in the solid films is attributed to the presence of low-energy traps, possibly low concentrations of molecular aggregates of the OPhBTDT2 moieties, although no spectral evidence was found for their existence. The absence of an affect by the TPA groups on the decay times of the OPhBTDT2 singlet and triplet excitons is consistent with the migration of electronic energy to the non-emissive traps being much more efficient than the photo-induced oxidation of the TPA groups.

The extensive quenching of photoluminescence from the homopolymer containing pendant OPhBTDT2 groups in a blended film containing 50% (w/w) of the electron acceptor $PC_{61}BM$ is attributed to photo-induced reduction of $PC_{61}BM$ by the OPhBTDT2 singlet excitons. Evidence for the formation of the associated charge carriers was obtained from nanosecond transient absorbance measurements, and analysis of the decay kinetics of the transient absorbance signals of these species indicates a substantial contribution to bimolecular recombination by slow thermal activation out of an exponential distribution of localised (trapped) states. Evidence was also obtained from the transient absorption measurements suggesting extensive phase separation in the blended film. The performance of OPV devices based on this blend delivered low PCE, despite the slow bimolecular charge recombination, which may be the result of substantial phase separation and possibly low mobility of holes in the homopolymer phase.

Acknowledgements

This research was funded through the Flexible Electronics Theme of the CSIRO Future Manufacturing Flagship, and was also supported by the Victorian Organic Solar Cell Consortium (established through a Research and Development Grant from the Victorian Government Department of Primary Industries), an International Science Linkage Grant (CG100059) from the Australian Government (Department of Innovation, Industry, Science and Research), and a Post-doctoral Fellowship awarded to MH by CSIRO's Office-of-the-Chief Executive. The authors are grateful to Dr. Jacek Jacieniak for conducting the OPV performance measurements.

Appendix A. Supplementary data

Supplementary data associated with this article can be found, in the online version, at doi:10.1016/j.jphotochem.2011.03.026.

References

[1] K. Sivula, Z.T. Ball, N. Watanabe, J.M.J. Frechet, Adv. Mater. 18 (2006) 206–210.
[2] M. Jeffries-El, G. Sauve, R.D. McCullough, Macromolecules 38 (2005) 10346–10352.
[3] G. Sauve, R.D. McCullough, Adv. Mater. 19 (2007) 1822–1825.
[4] J.S. Liu, E. Sheina, T. Kowalewski, R.D. McCullough, Angew. Chem. Int. Ed. 41 (2001) 322–329.
[5] M. Behl, E. Hattemer, M. Brehmer, R. Zentel, Macromol. Chem. Phys. 203 (2002) 503–510.
[6] M. Behl, R. Zentel, Macromol. Chem. Phys. 205 (2004) 1633–1643.
[7] S. Barrau, T. Heiser, F. Richard, C. Brochon, C. Ngov, K. van de Wetering, G. Hadzioannou, D.V. Anokhin, D.A. Ivanov, Macromolecules 41 (2008) 2701–2710.
[8] C. Yang, J.K. Lee, A.J. Heeger, F. Wudl, J. Mater. Chem. 19 (2009) 5416–5423.
[9] B. de Boer, U. Stalmach, P.F. van Hutten, C. Melzer, V.V. Krasnikov, G. Hadzioannou, Polymer 42 (2001) 9097–9109.
[10] A. de Cuendias, M. Le Hellaye, B. Lecommandoux, E. Cloutet, H. Cramail, J. Mater. Chem. 15 (2005) 3264–3267.
[11] S. Rajaram, P.B. Armstrong, B.J. Kim, J.M.J. Frechet, Chem. Mater. 21 (2009) 1775–1777.
[12] S.M. Lindner, M. Thelakkat, Macromolecules 37 (2004) 8832–8835.
[13] U. Stalmach, B. de Boer, C. Videlot, P.F. van Hutten, G. Hadziioannou, J. Am. Chem. Soc. 122 (2000) 5464–5472.
[14] C.C. Zhao, Y. Zhang, S.L. Pan, L. Rothberg, M.K. Ng, Macromolecules 40 (2007) 1816–1823.
[15] M. Melucci, L. Favaretto, C. Bettini, M. Gazzano, N. Camaioni, P. Maccagnani, P. Ostoja, M. Monari, G. Barbarella, Chem. Eur. J. 13 (2007) 10046–10054.
[16] P. Sonar, S.P. Singh, S. Sudhakar, A. Dodabalapur, A. Sellinger, Chem. Mater. 20 (2008) 3184–3190.
[17] P.M. Beaujuge, J. Subbiah, K.R. Choudhury, S. Ellinger, T.D. McCarley, F. So, J.R. Reynolds, Chem. Mater. 22 (2010) 2093–2106.
[18] M. Häussler, P. Lok, M. Chen, J. Jasieniak, R. Adhikari, S.P. King, S.A. Haque, C.M. Forsyth, K. Winzenberg, S.E. Watkins, E. Rizzardo, G.J. Wilson, Macromolecules 43 (2010) 7101–7110.
[19] V. Barone, M. Cossi, J. Phys. Chem. A 102 (1998) 1995–2001.
[20] A.L. Speelman, J.G. Gillmore, J. Phys. Chem. A 112 (2008) 5684–5690.
[21] M. Cossi, V. Barone, J. Chem. Phys. 115 (2001) 4708–4717.
[22] J. Fortage, A. Scarpaci, L. Viau, Y. Pellegrin, E. Blart, M. Falkenstrom, L. Hammarstrom, I. Asselberghs, R. Kellens, W. Libaers, K. Clays, M.P. Eng, F. Odobel, Chem. Eur. J. 15 (2009) 9058–9067.
[23] J.M. Tour, R.L. Wu, Macromolecules 25 (1992) 1901–1907.
[24] R.D. Gordon, R.F. Yang, J. Mol. Spectrosc. 39 (1971) 295–320.
[25] D.L. Gerrard, W.F. Maddams, P.J. Tucker, Spectrochim. Acta Part a-Mol. Biomol. Spectrosc. 34 (1978) 1225–1230.

[26] J.R. Lakowicz, Principles of Fluorescence Spectroscopy, 3rd ed., Springer, Singapore, 2006, p. 208.
[27] J.S. de Melo, L.M. Silva, M. Kuroda, J. Chem. Phys. 115 (2001) 5625–5636.
[28] V. Wintgens, P. Valat, F. Garnier, J. Phys. Chem. 98 (1994) 228–232.
[29] S.S. Emmi, M. D'Angelantonio, G. Beggiato, G. Poggi, A. Geri, D. Pietropaolo, G. Zotti, Radiat. Phys. Chem. 54 (1999) 263–270.
[30] P. Camilleri, A. Dearing, D.J. Colehamilton, P. Oneill, J. Chem. Soc.-Perkin Trans. 2 (1986) 569–572.
[31] R.J. Lipert, S.D. Colson, A. Sur, J. Phys. Chem. 92 (1988) 183–185.
[32] G. Porter, M.W. Windsor, Proc. Roy. Soc. Lond. Ser. a-Math. Phys. Sci. 245 (1958) 238–258.
[33] N.J. Turro, V. Ramamurthy, J.C. Scaiano, Principles of Molecular Photochemistry: An Introduction University Science Books, 2009, pp. 414–416.
[34] E.N. Bodunov, M.N. Berberan-Santos, J.M.G. Martinho, Chem. Phys. 316 (2005) 217–224.
[35] J. Clark, C. Silva, R.H. Friend, F.C. Spano, Phys. Rev. Lett. 98 (2007) 206406.
[36] P. Bojarski, Chem. Phys. Lett. 278 (1997) 225–232.
[37] S. Yamamoto, J. Guo, H. Ohkita, S. Ito, Adv. Funct. Mater. 18 (2008) 2555–2562.
[38] J.W. Arbogast, A.P. Darmanyan, C.S. Foote, Y. Rubin, F.N. Diederich, M.M. Alvarez, S.J. Anz, R.L. Whetten, J. Phys. Chem. 95 (1991) 11–12.
[39] D.M. Guldi, H. Hungerbuhler, E. Janata, K.D. Asmus, J. Phys. Chem. 97 (1993) 11258–11264.
[40] S. Cook, H. Ohkita, J.R. Durrant, Y. Kim, J.J. Benson-Smith, J. Nelson, D.D.C. Bradley, Appl. Phys. Lett. 89 (2006) 101128.
[41] H. Ohkita, S. Cook, Y. Astuti, W. Duffy, S. Tierney, W. Zhang, M. Heeney, I. McCulloch, J. Nelson, D.D.C. Bradley, J.R. Durrant, J. Am. Chem. Soc. 130 (2008) 3030–3042.
[42] I. Montanari, A.F. Nogueira, J. Nelson, J.R. Durrant, C. Winder, M.A. Loi, N.S. Sariciftci, C. Brabec, Appl. Phys. Lett. 81 (2002) 3001–3003.
[43] J. Nelson, Phys. Rev. B 67 (2003) 155209.
[44] A.F. Nogueira, I. Montanari, J. Nelson, J.R. Durrant, C. Winder, N.S. Sariciftci, J. Phys. Chem. B 107 (2003) 1567–1573.
[45] T.M. Clarke, F.C. Jamieson, J.R. Durrant, J. Phys. Chem. C 113 (2009) 20934–20941.
[46] H.X. Luo, M. Fujitsuka, Y. Araki, O. Ito, P. Padmawar, L.Y. Chiang, J. Phys. Chem. B 107 (2003) 9312–9318.
[47] R.V. Bensasson, E. Bienvenue, C. Fabre, J.M. Janot, E.J. Land, S. Leach, V. Leboulaire, A. Rassat, S. Roux, P. Seta, Chem. Eur. J. 4 (1998) 270–278.
[48] S. Cook, H. Ohkita, Y. Kim, J.J. Benson-Smith, D.D.C. Bradley, J.R. Durrant, Chem. Phys. Lett. 445 (2007) 276–280.
[49] H.C. Kim, S.M. Park, W.D. Hinsberg, Chem. Rev. 110 (2010) 146–177.
[50] D.J. van den Heuvel, I.Y. Chan, E.J.J. Groenen, J. Schmidt, G. Meijer, Chem. Phys. Lett. 231 (1994) 111–118.